

# A NEW APPROACH FOR PREDICTING THE FATIGUE STRENGTH OF STEELS AND ALUMINIUM ALLOYS IN HIGH & GIGA CYCLE REGIMES

A.M.A.C.S. Bandara,  
Department of Civil Engineering, University of Peradeniya  
E-mail: bandara@civil.pdn.ac.lk

P.B.R. Dissanayake  
Department of Civil Engineering, University of Peradeniya  
E-mail: ranjith@civil.pdn.ac.lk

U.I. Dissanayake  
Department of Civil Engineering, University of Peradeniya  
E-mail: udissa@pdn.ac.lk

S.A.S.C. Siriwardane  
Department of Mechanical and Structural Engineering and Material Science, Faculty of Science and Technology, University of Stavanger, N-4036 Stavanger, Norway  
E-mail: sasc.siriwardane@uis.no

## Abstract

Since 1990s various methods have been proposed by researchers to estimate the fatigue strengths of metals at gigacycle fatigue regime (number of cycles  $> 10^8$ ). As testing of metals in the gigacycle regime requires much time and sophisticated equipment, obtaining experimental fatigue strengths at gigacycle regime is difficult. Therefore, fatigue strength prediction methods are very important. However, the available prediction methods are complicated and require parameters which are not easily tested. Therefore, it is necessary to discover simple but reliable prediction methods that require few and easily obtainable material parameters.

In this study, a new model for predicting the fatigue strength of steels at high and gigacycle fatigue regimes is first proposed. A good global relationship between the ultimate tensile strength, the fatigue strength and the number of cycles to failure is obtained after analyzing more than 80 heats of experimental results of 45 steels and 9 aluminium alloys. Using this global relationship, secondly, a model is proposed for predicting the fatigue strength of steels and alloys.

**Keywords:** fatigue strength, giga cycle regime, Vicker's hardness, internal inclusions, cyclic stresses

# 1. Introduction

Fatigue fracture is common for all metals subjected to cyclic loading. When the cyclic stresses are high, fatigue fracture occurs at less loading cycles and vice versa. Since the findings in 1990s that there is no endurance limit for metals (Bathias et al.), a lot of research work has been done to develop stress life (S-N) curves and methods to predict fatigue strengths of metallic materials in the gigacycle regime.

Sample testing in the gigacycle regime requires sophisticated equipment, precise temperature control techniques and much time. As a result, obtaining fatigue strengths ( $\sigma_w$ ) using experiments is difficult. Therefore it is very important to develop fatigue strength prediction models with easily tested material properties such as the ultimate tensile strength ( $\sigma_u$ ) and Vickers hardness (Hv). The available prediction methods such as the Murakami model or modified Murakami model require mechanical properties of metals and sizes of non metallic inclusions ( $\sqrt{area}$ ) in the metal for predicting the fatigue strength. There are other methods that have been developed using fracture energy concepts, stress intensity factors etc., which also require parameters not easily available.

The Murakami model was developed using  $\sqrt{area}$  and Hv as important parameters for predicting fatigue strength. Liu et al., Bathias et al., Mayor et al., and Chapetti et al., have proposed various modifications to the Murakami model in order to widen its applicability.

The fatigue fracture at gigacycle regime is mainly caused by non metallic inclusions inside metals as mentioned by Liu et al., Bathias et al., and Chapetti et al., etc. There may be many external and internal defects in metals though usually it is one defect that causes the failure in the gigacycle regime. The size of the inclusion and/or the optically dark area (ODA) formed around the inclusion should exceed the threshold size in order to start the propagation of a crack. Due to the variability of sizes of inclusions and defects in metals and stress concentrations at these defects, it is difficult to predict a definite size of an inclusion or defect which causes the failure. However, using the theories and findings on the subject, a reasonable critical inclusion size could be estimated. This estimated critical inclusion size could be used to predict the fatigue strength of a material with reasonable accuracy.

This study was carried out to propose a simple and reasonably accurate model for predicting the fatigue strength of high strength steels;  $\sigma_u > 1200$  Mpa and medium (and low) strength steels;  $\sigma_u < 1200$  Mpa with a carbon equivalency value (CEV) less than 1% in the gigacycle regime. Experimental results of 45 steels and 9 aluminium alloys published by several research groups were used in the study. The parameters used in the proposed simplified model are  $\sigma_u$ , Hv and  $N_f$  (number of cycles to failure). The study was further extended to propose a global fatigue strength model for steels and alloys. The important feature of this is that the main parameters used in the global simplified model are only  $\sigma_u$  and  $N_f$ .

## 2. A simplified model for fatigue strength

According to Murakami et al., for mode I (opening mode) fatigue cracks, the maximum stress intensity factor ( $K_{I-max}$ ) at an internal inclusion and an external defect are given by  $0.50\sigma_o\sqrt{(\pi\sqrt{area})}$  and  $0.65\sigma_o\sqrt{(\pi\sqrt{area})}$  respectively, where  $\sigma_o$  is the applied stress. Microscopic examinations of fracture surfaces of test samples show both the external and internal failures at high and gigacycle regimes. Therefore, the average of the above two values could give a reasonable prediction for  $K_{I-max}$ , that is;

$$K_{I-max} = 0.57\sigma_o\sqrt{(\pi\sqrt{area})} \quad (1)$$

Where,  $K_{I-max}$  is given in  $MPa\sqrt{m}$ ,  $\sigma_o$  is given in MPa, and  $\sqrt{area}$  is given in m.

As mentioned by Murakami et al., and Fuchs et al., the critical value of the stress intensity factor under which no cracks could initiate is approximately 1.8~2.0  $MPa\sqrt{m}$ . Then the minimum crack size of any internal inclusion or surface defect could be approximated to;

$$\sqrt{area} = 1.9^2 / \{(0.57\sigma_o)^2\pi\} \quad (2)$$

where,  $K_{I-max}$  is taken as the average of the given values; 1.9  $MPa\sqrt{m}$ .

Equation (2) shows that the  $\sqrt{area}$  varies with the applied stress and that  $\sigma_o^2$  is inversely proportional to  $\sqrt{area}$ . Once the applied stress exceeds the fatigue strength limit at the crack, the crack must start propagating. Therefore, applying fatigue strength (at a given number of cycles) for  $\sigma_o$  in the equation (2) should give the minimum critical crack size.

The upper bound fatigue strength of a material in the high cycle regime ( $\sigma_{wo}$ ) is approximated to  $0.5\sigma_u$  (as proposed by Murakami et al.). Therefore, applying  $0.5\sigma_u$  for  $\sigma_o$  in the equation (2) and simplifying the equation, the approximate minimum critical crack size can be expressed as;

$$\sqrt{area} = 14/\sigma_u^2 \quad (3)$$

where, the unit of  $\sqrt{area}$  is in m.

The modified Murakami model by Wang et al., for fatigue strength at  $R=-1$  that includes the effect of failure number of cycles is given by;

$$\sigma_w = \beta(Hv+120)/(\sqrt{area})^{1/6} \quad (4)$$

where,  $\beta = \beta_1 - \beta_2 \text{Log}N_f$  in which  $\beta_1$  and  $\beta_2$  are constants for materials and location of defects (inclusions). The unit of  $\sigma_w$  is in MPa, Hv is in  $\text{kgf/mm}^2$  and  $\sqrt{area}$  is in  $\mu\text{m}$ .

Substituting for  $\sqrt{\text{area}}$  with the relevant unit from equation (3) in equation (4) and introducing proposed global values for  $\beta_1$  and  $\beta_2$  (2.41 and 0.109 respectively), the fatigue strength at any failure cycles  $N_f > 10^6$  is given by;

$$\sigma_w = (1/1000)(Hv+120)(155-7\text{Log}N_f) \sigma_u^{1/3} \quad (5)$$

where, the units of the terms of equation (5) are the same as those in equation (4).

If one of the two parameters  $\sigma_u$  or Hv is not available, the following relationship may be used to evaluate the unavailable parameter.

$$\sigma_u = 3.32Hv \quad (6)$$

where, the unit of  $\sigma_u$  is in MPa and that of Hv is in kgf/mm<sup>2</sup>. The constant 3.32 is the mean value obtained for the materials used in this study (Figure A 1 in the Appendix).

As the values of  $\sigma_u$  and Hv are easily obtainable for any metal, this equation is simple. The range of  $N_f$  in the equation (5) is valid from  $10^6$  cycles as verified using experimental mean S-N curves. Most importantly, the fatigue strength predictions at a given number of cycles for 96% of the heats of steels used in the study are within 20% error margin and 80% of the predictions are within 15% error margin (Figure 1 and Appendix: Table A 2).

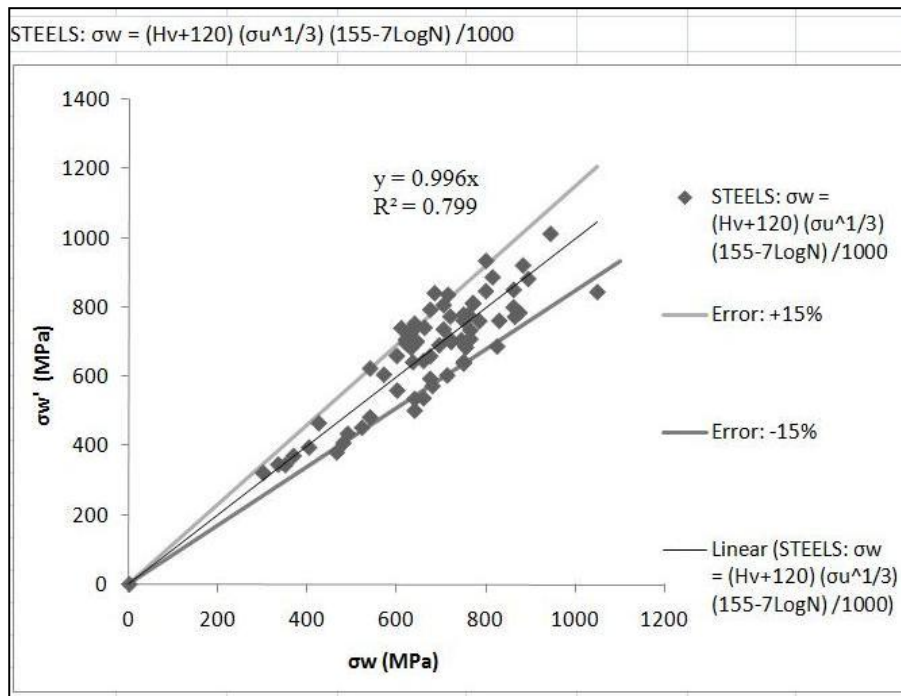


Figure 1.  $\sigma_w'$  vs  $\sigma_w$  and 15% error margin for predictions of equation (5)

### 3. Material details and the method of analysis

Materials used to verify the equation (5) are medium and high strength steels tested and published by various research groups. The loading conditions are; test loading with  $R=-1$ , axial loading and rotating bending with loading frequencies of 20Hz-150Hz in the high cycle regime and 20kHz in the gigacycle regime. The mechanical properties and carbon & alloy compositions of the materials are given in Table A 1 (Appendix).

One to three  $N_f$  values and relevant  $\sigma_w$  were obtained for each material subject to details available in published mean S-N curves.  $N_f$  values used are above  $10^6$  cycles.

### 4. Results and discussion

The fatigue strengths obtained from mean S-N curves and the calculated fatigue strengths  $\sigma_w'$  using equation (5) are given in Table A 2 (Appendix). Figure 1 shows the graph of  $\sigma_w$  vs  $\sigma_w'$  with 15% error margins.

During the analysis, it was observed that high carbon steels ( $CEV > 1\%$ ) and steels with a fatigue strength above 900MPa at gigacycle regime deviate from the error margins when equation (5) is used.

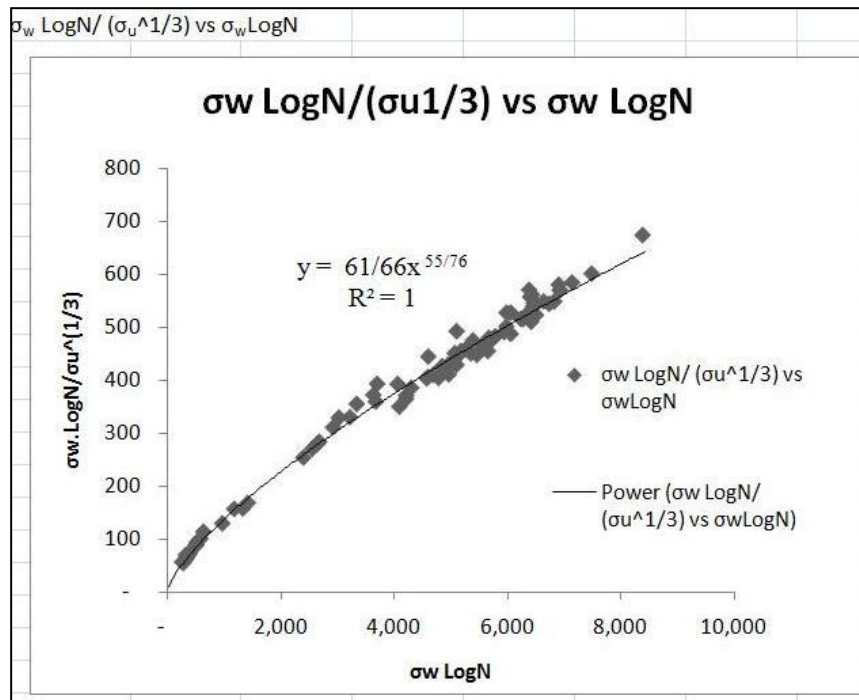


Figure 2. Relationship between  $\sigma_w$ ,  $\sigma_u^{1/3}$  and  $N_f$  for steels and aluminium alloys

Equation (5) is a relationship of  $\sigma_w$  and  $\sigma_u^{1/3}$ . Further analysis of  $\sigma_w$ ,  $N_f$  and  $\sigma_u$  showed an empirical relationship between  $\sigma_w$  and  $\sigma_u^{1/3}$ , when plotted for  $(\sigma_w \text{Log}N_f / \sigma_u^{1/3})$  vs  $(\sigma_w \text{Log}N_f)$  as

given in Figure 2. Nine aluminium alloys were also added to the analysis to include the impact of  $\sigma_u < 650\text{MPa}$  (Table A 3 in the Appendix). The simplified form of this relationship is given by;

$$\sigma_w = \gamma \sigma_u^\eta / \text{Log} N_f \quad (7)$$

where,  $\gamma$  and  $\eta$  are found as 0.752 and 1.206 for steels and aluminium alloys. The unit of both  $\sigma_w$  and  $\sigma_u$  are in MPa.  $N_f$  is in cycles and greater than  $10^6$ .

Equation (7) is proposed as the most simplified model for predicting the fatigue strength of steels and alloys. Figure 3 shows  $\sigma_w'$  vs  $\sigma_w$  with the 20% error margins that verify the accuracy of the predictions of equation (7).

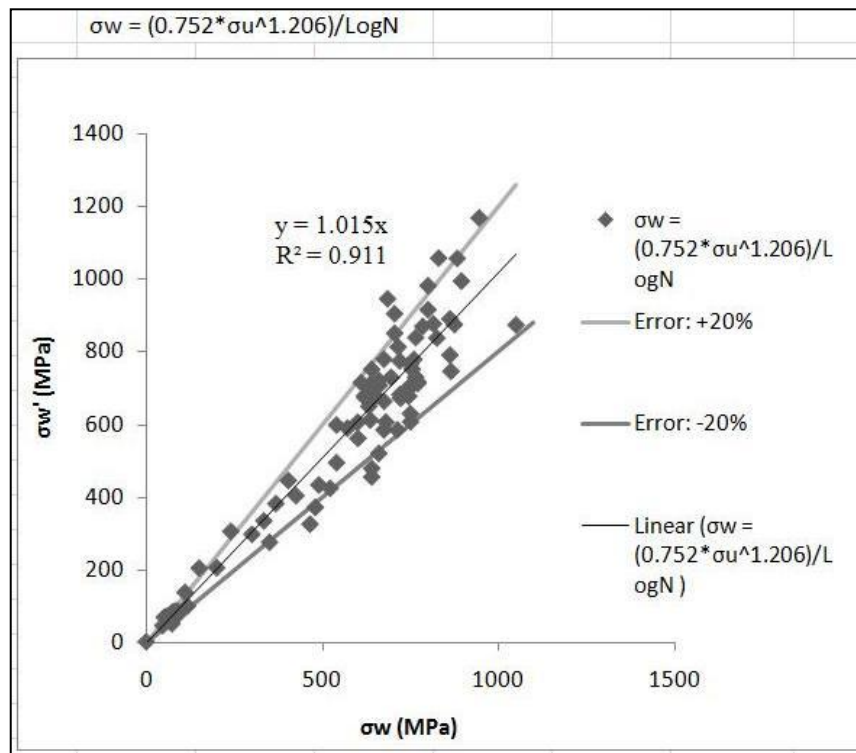


Figure 3.  $\sigma_w'$  vs  $\sigma_w$  and 20% error margin for predictions of equation (7)

## 5. Conclusions

The two main conclusions of the study are as follows.

1. A simplified model for predicting the fatigue strength at a given number of loading cycles ( $N_f > 10^6$ ) for medium and high strength steels is proposed. The distinctive feature of the model is that it only consists of  $\sigma_u$ ,  $H_v$  and  $N_f$ . The accuracy of the predictions is verified using 45 medium and high strength steels.

2. An empirical global model is introduced for predicting the fatigue strength of steels and alloys at a given number of loading cycles ( $N_f > 10^6$ ). This model is proposed as the most simplified model as it only requires  $\sigma_u$  and  $N_f$  for predicting the fatigue strength. The accuracy of the prediction is verified using 45 medium and high strength steels and 9 aluminium alloys.

## Acknowledgement

Authors would like to thank the National Research Council of Sri Lanka (No. 11-106).

## Reference

Bathias C (1999) "There is no infinite fatigue life in metallic materials", *Fatigue & fracture of engineering materials & structures*, 22(7) : 559-565.

Chapetti M D (2006) "Ultra-high cycle fatigue in high strength steels", *Conamet/SAM*, (available online: [www.materiale-sam.org.ar/sitro/biblioteca/g6.pdf](http://www.materiale-sam.org.ar/sitro/biblioteca/g6.pdf) [accessed 12/09/2012]).

Duan Z, Ma X F, Shi H J, Murai R, Yanagisawa E (2011) "Gigacycle fatigue behavior of two SNCM439 steels with different tensile strengths", *Acta Mech. Sin.*, 27(5) : 778-784.

Fuchs H O, Stephens R I (1980), *Metal fatigue in engineering*, first ed., John Willy, New York.

Furuya Y, Matsuoka S, Abe T, Yamaguchi K (2002) "Gigacycle properties of high-strength low-alloy steel at 100Hz, 600Hz and 20kHz", *Scripta Materialia*, 46 : 157-162.

Garcia I M, Montiel D G, Bathias C (2008) "Fatigue life assessment of high-strength low alloy steel at high frequency", *The Arabian J. of Sci. and Engg.*, 33 : 237-247.

Li Y D, Chen S M, Liu Y B, Yang Z G, Li S X, Hui W J, Weng Y Q (2010) "The characteristics of granular-bright facet in hydrogen pre-charged and uncharged high strength steels in the very high cycle fatigue regime", *J. Mater. Sci.*, 45 : 831-841.

Li Y D, Yang Z G, Li S X, Liu Y B, Chen S M, Hui W J, Weng Y Q (2009) "Effect of hydrogen on fatigue strength of high-strength steels in the VHCF regime", *Advance Engng. Materials*, 11(7) : 561-567.

Liu Y B, Li Y D, Yang Z G, Chen S M, Hui W J, Weng Y Q (2010) “Prediction of the S-N curves of high strength steels in the very high cycle fatigue regime”, *Int. J. of Fatigue*, 32 : 1351-1357.

Liu Y B, Yang Z G, Li Y D, Chen S M, Li S X, Hui W J, Weng Y Q (2009) “Dependence of fatigue strength on inclusion size for high strength steels in very high cycle fatigue regime”, *Mat. Sci. and Engineering A*, 517 : 180-184.

Mayer H, Papakyriacou M, Zettl B, Stanzl-Tschegg S E (2003) “Influence of porosity on the fatigue limit of die cast magnesium and aluminium alloys”, *Int. J. of Fatigue*, 25 : 245-256.

Murakami Y (2002) *Metal fatigue: effects of small defects and non metallic inclusions*, first ed., Elsevier, Oxford.

Murakami Y, Endo M (1986) “Effects of hardness and crack geometries on  $\Delta K_{th}$  of small cracks emanating from small defects”, In: Miller K J, de los Rios E R (Eds.), *The behavior of short fatigue cracks*, Mechanical Engineering Publications, London, pp.275-293.

Nishijima S, Kanazawa K (1999) “Stepwise S-N curve and fish-eye failure in gigacycle fatigue”, *Fatigue Fract. Engng. Mater. Struct.*, 22 : 601-607.

NRIM (2005) *Fatigue datasheet 97*, (available online: <http://mits.nism.go.jp/en/./html> [accessed on 30/10/2012])

NRIM (2008) *Fatigue datasheet 104*, (available online: <http://mits.nism.go.jp/en/./html> [accessed on 30/10/2012])

NRIM (1978) *Fatigue datasheet 44*, (available online: <http://mits.nism.go.jp/en/./html> [accessed on 30/10/2012])

Sonsino C M (2007) “Course of SN curves especially in the high-cycle fatigue regime with regard to component design and safety”, *Int. J. of Fatigue*, 29 : 2246-2258.

Wang Q Y, Berard Y J, Dubarre A, Baudry G, Rathery S, Bathias C (1999) “Gigacycle fatigue of ferrous alloys”, *Fatigue fract. Engng. Mater. Struct.*, 22 : 667-672.

Wang Y Q, Bathias C, Kawagoishi N, Chen Q (2002) “Effect of inclusion on subsurface crack initiation and gigacycle fatigue strength”, *Int. J. of Fatigue*, 24 : 1269-1274.

Yu Y, Gu J L, Xu L, Shou F L, Bai B Z, Liu Y B (2010) “Very high cycle fatigue behaviors of Mn-Si-Cr series Bainite/Martensite dual phase steels”, *Materials and Design*, 31 : 3067-3072.

## Appendix

*Table A 1. Mechanical properties & carbon and alloy composition of steels*

<i>Steel</i>	<i>Carbon and alloy composition</i>	$\sigma_u$ (Mpa)	$H_v$ (kgf/mm <sup>2</sup> )	<i>Reference</i>
<i>KSFA80</i>	<i>As per reference 8</i>	800	275	8
<i>S40C</i>	<i>0.41C,0.74Mn,0.12Cr</i>	857	286	12
<i>S55C / 550C (F)</i>	<i>0.57C,0.74Mn,0.12Cr,0.01Ni,0.02Cu</i>	957	314	13
<i>D38MSV5S</i>	<i>0.38C,1.23Mn,0.02Mo,0.09V,0.06Ni,0.06Cu</i>	877	246	20
<i>KSFA110</i>	<i>As per reference 8</i>	1,100	360	8
<i>SCM440</i>	<i>0.42C,0.80Mn,1.16Cr,0.16Mo,0.02Ni,0.01Cu</i>	1,134	367	14
<i>SUP7 (1)</i>	<i>As per reference 8</i>	1,423	441	8
<i>Mn-Si-Cr-3</i>	<i>0.22C,2.25Mn,0.89Cr,0.36Mo,1.15Ni</i>	1,451	453	9
<i>42CrMo4-RC</i>	<i>0.41C,0.84Mn,1.03Cr,0.16Mo,0.19Ni</i>	1,485	450	11,6
<i>G</i>	<i>0.24C,0.77Mn,1.2Cr</i>	1,489	414	15
<i>1CrMo steel</i>	<i>1Cr 0.2Mo</i>	1,502	450	16
<i>42CrMo4-UC</i>	<i>0.43C,0.83Mn,1.03Cr,0.22Mo,0.17Ni</i>	1,530	465	11,6
<i>F50CrV4</i>	<i>0.51C,0.95Mn,1.10Cr,0.13V</i>	1,540	449	17
<i>F50CrV4</i>	<i>0.51C,0.95Mn,1.10Cr,0.13V</i>	1,540	440	15
<i>Mn-Si-Cr-1-4</i>	<i>0.21C,0.22Mn,0.62Cr</i>	1,547	483	9
<i>G50CrV4 (G-QT)</i>	<i>0.51C,0.95Mn,1.10Cr,0.13V</i>	1,550	450	15
<i>Mn-Si-Cr-1-3</i>	<i>0.21C,0.22Mn,0.62Cr</i>	1,581	494	9
<i>Mn-Si-Cr-2</i>	<i>0.23C,2.24Mn,0.68Cr</i>	1,640	513	9
<i>50CrV4-1</i>	<i>0.51C,0.93Mn,1.02Cr</i>	1,680	506	5
<i>CrSi (54SC6)</i>	<i>0.54C,0.63Mn,0.64Cr,0.06Ni</i>	1,692	510	11,6
<i>SNCM439 - B</i>	<i>0.42C,0.84Mn,0.79Cr,0.15Mo,1.6Ni,0.1Cu</i>	1,710	534	18
<i>SUP12</i>	<i>As per reference 8</i>	1,720	516	8
<i>54SiCrV6</i>	<i>0.56C,0.70Mn,0.65Cr,0.15V</i>	1,729	515	5
<i>SUP7 (2)</i>	<i>As per reference 8</i>	1,730	528	8
<i>60Si2Mn-1</i>	<i>0.59C,0.70Mn</i>	1,732	511	5
<i>54SiCr6</i>	<i>0.56C,0.70Mn,0.65Cr</i>	1,743	500	5
<i>60Si2CrV-1</i>	<i>0.59C,0.53Mn,0.96Cr,0.11V,0.09Ni</i>	1,750	538	5
<i>50CrV4-2</i>	<i>0.51C,0.95Mn,1.10Cr,0.13V</i>	1,750	519	5
<i>60Si2Cr</i>	<i>0.56C,0.44Mn,0.74Cr</i>	1,753	513	5
<i>SWOSC-V</i>	<i>As per reference 8</i>	1,764	528	8
<i>CrSi (54SC7)</i>	<i>0.56C,0.70Mn,0.70Cr</i>	1,800	500	11,6
<i>CrV (60CrV2)</i>	<i>0.51C,0.85Mn,0.95Cr,0.15V</i>	1,800	437	11,6
<i>60Si2CrV-2</i>	<i>0.59C,0.53Mn,0.96Cr,0.11V,0.09Ni</i>	1,804	543	5
<i>SUP12 (SUP-QT)</i>	<i>0.53C,0.69Mn,0.74Cr,0.11V</i>	1,815	604	17,15,8
<i>40CrNiMo</i>	<i>0.41C,0.80Mn,0.76Cr</i>	1,820	540	5
<i>SUP12</i>	<i>0.53C,0.69Mn,0.74Cr,0.02Ni</i>	1,825	604	5
<i>SUP10M 10M3</i>	<i>As per reference 11,6</i>	1,836	550	11,6
<i>SUP10M 10M6</i>	<i>As per reference 11,6</i>	1,849	554	11,6
<i>SUP10M</i>	<i>As per reference 8</i>	1,850	554	8
<i>60Si2CrV-5</i>	<i>0.56C,0.65Mn,1.10Cr,0.14V</i>	1,925	562	5
<i>SCM435H</i>	<i>As per reference 8</i>	1,950	564	8
<i>60Si2CrV-6</i>	<i>0.59C,0.60Mn,1.09Cr,0.11V,0.05Ni</i>	1,954	558	5
<i>60Si2CrV-4</i>	<i>0.58C,0.47Mn,0.99Cr,0.12V</i>	1,955	571	5
<i>SNCM439</i>	<i>0.41C,0.74Mn,0.74Cr,0.22Mo,1.84Ni</i>	1,955	598	19
<i>NHS1</i>	<i>0.44C,0.73Mn,0.92Cr</i>	2,025	600	5

Table A 2. Experimental fatigue strength, calculated fatigue strength and the percentage error

Steel	Reference	N (cycles)	$\sigma_w$ (Mpa)	$\sigma_{w0} =$ $0.5\sigma_u$ (Mpa)	$\sqrt{\text{area from}}$ equation (3) ( $\mu\text{m}$ )	$\sigma_w'$ from equation (5) (Mpa)	Error ( $\sigma_w' -$ $\sigma_w$ ) / $\sigma_w'$ (%)
KSFA80	8	5.00E+08	350	400	21.88	345	-1%
S40C/550C (B)	12	1.00E+06	490	429	19.06	436	-11%
S40C/550C (B)	12	1.00E+07	480	429	19.06	409	-15%
S40C/550C (B)	12	1.00E+08	465	429	19.06	382	-18%
D38MSV5S	13	1.00E+06	403	439	18.20	396	-2%
D38MSV5S	13	1.00E+07	368	439	18.20	372	1%
D38MSV5S	13	1.00E+08	334	439	18.20	347	4%
D38MSV5S	13	1.00E+09	300	439	18.20	322	7%
S55C / 550C (F)	20	1.00E+06	540	479	15.29	484	-10%
S55C / 550C (F)	20	1.00E+07	522	479	15.29	454	-13%
KSFA110	8	5.00E+08	425	550	11.57	467	10%
SCM440/550C (C)	14	1.00E+06	680	567	10.89	574	-16%
SCM440/550C (C)	14	1.00E+07	660	567	10.89	539	-18%
SCM440/550C (C)	14	1.00E+08	640	567	10.89	503	-21%
SUP7 (1)	8	1.00E+08	540	712	6.91	625	16%
SUP7 (2)	8	1.00E+10	640	712	6.91	537	-16%
Mn-Si-Cr-3	9	1.00E+08	636	726	6.65	643	1%
42CrMo4 RC	11,6	1.00E+06	765	743	6.35	736	-4%
42CrMo4 RC	11,6	1.00E+08	750	743	6.35	644	-14%
G	15	1.00E+07	660	745	6.31	647	-2%
G	15	1.00E+09	601	745	6.31	561	-7%
1CrMo steel	16	1.00E+06	705	751	6.20	738	5%
1CrMo steel	16	1.00E+07	695	751	6.20	693	0%
1CrMo steel	16	5.00E+07	675	751	6.20	661	-2%
42CrMo4 UC	11,6	1.00E+06	785	765	5.98	762	-3%
42CrMo4 UC	11,6	4.00E+08	750	765	5.98	639	-15%
F50CrV4	17	1.00E+09	713	770	5.90	605	-15%
F50CrV4	15	1.00E+07	755	770	5.90	686	-9%
F50CrV4	15	1.00E+09	675	770	5.90	595	-12%
Mn-Si-Cr-1-4	9	1.00E+08	635	774	5.85	691	9%
G50CrV4	15	1.00E+09	571	775	5.83	607	6%
Mn-Si-Cr-1-3	9	1.00E+06	705	791	5.60	809	15%
Mn-Si-Cr-1-3	9	1.00E+08	620	791	5.60	709	14%
Mn-Si-Cr-2	9	1.00E+06	685	820	5.21	844	23%
Mn-Si-Cr-2	9	1.00E+08	635	820	5.21	739	16%
50CrV4-1	5	1.00E+09	632	840	4.96	685	8%
CrSi (54SC6)	11,6	1.00E+06	800	846	4.89	849	6%
CrSi (54SC6)	11,6	5.00E+08	745	846	4.89	707	-5%
SNM439 - B	18	1.00E+06	895	855	4.79	885	-1%

<i>SNCM439 - B</i>	18	1.00E+08	865	855	4.79	775	-10%
<i>SUP12</i>	8	1.00E+08	640	860	4.73	755	18%
<i>54SiCrV6</i>	5	1.00E+09	722	865	4.68	702	-3%
<i>SUP7</i>	8	1.00E+10	600	865	4.68	661	10%
<i>60Si2Mn-1</i>	5	1.00E+09	621	866	4.67	698	12%
<i>54SiCr6</i>	5	5.00E+08	745	872	4.61	703	-6%
<i>60Si2CrV-1</i>	5	1.00E+09	632	875	4.57	730	15%
<i>50CrV4-2</i>	5	1.00E+09	720	875	4.57	709	-2%
<i>60Si2Cr</i>	5	1.00E+09	645	877	4.56	703	9%
<i>SWOSC-V</i>	8	1.00E+08	720	882	4.50	776	8%
<i>CrSi (54SC7)</i>	11,6	1.80E+07	875	900	4.32	787	-10%
<i>CrSi (54SC7)</i>	11,6	5.00E+08	765	900	4.32	710	-7%
<i>CrV (60CrV2)</i>	11,6	1.00E+06	830	900	4.32	764	-8%
<i>CrV (60CrV2)</i>	11,6	3.80E+07	825	900	4.32	689	-17%
<i>60Si2CrV-2</i>	5	1.00E+09	662	902	4.30	743	12%
<i>SUP12 (SUP-QT)</i>	17,15,8	1.00E+07	800	908	4.25	937	17%
<i>SUP12 (SUP-QT)</i>	17,15,8	1.00E+09	771	908	4.25	813	5%
<i>40CrNiMo</i>	5	1.00E+09	610	910	4.23	742	22%
<i>SUP12</i>	5	1.00E+09	771	913	4.20	814	6%
<i>SUP10M 10M3</i>	11,6	2.00E+07	862	918	4.15	853	-1%
<i>SUP10M 10M6</i>	11,6	1.60E+06	883	925	4.09	924	5%
<i>SUP10M</i>	8	2.00E+08	862	925	4.09	802	-7%
<i>60Si2CrV-5</i>	5	1.00E+09	750	963	3.78	781	4%
<i>SCM435H</i>	8	1.00E+08	1,050	975	3.68	847	-19%
<i>60Si2CrV-6</i>	5	1.00E+09	760	977	3.67	780	3%
<i>60Si2CrV-4</i>	5	1.00E+09	675	978	3.66	795	18%
<i>SNCM439</i>	19	1.00E+06	945	978	3.66	1,015	7%
<i>SNCM439</i>	19	1.00E+08	815	978	3.66	889	9%
<i>SNCM439</i>	19	1.00E+10	750	978	3.66	763	2%
<i>NHS1</i>	5	1.00E+09	715	1,013	3.41	838	17%

Table A 3. Aluminium alloys used in the study and  $\sigma_w'$  using equation (7) vs  $\sigma_w$

Material	Reference	$\sigma_u$ (Mpa)	Hv (kgf/mm <sup>2</sup> )	N (cycles)	$\sigma_w$ (Mpa)	$\sigma_w'$ from equation (7) (Mpa)	Error ( $(\sigma_w' - \sigma_w) / \sigma_w$ (%)
<i>AS21hp</i>	7	131	55	1.00E+05	70	54	-23%
<i>AS21hp</i>	7	131	55	1.00E+06	47	45	-5%
<i>AM60hp</i>	7	178	47	1.00E+05	82	78	-5%
<i>AM60hp</i>	7	178	47	1.00E+06	60	65	8%
<i>AE42hp</i>	7	184	57	1.00E+05	73	81	11%
<i>AE42hp</i>	7	184	57	1.00E+06	51	68	32%

AZ91hp	7	190	63	1.00E+05	81	84	4%
AZ91hp	7	190	63	1.00E+06	57	70	23%
AZ91 (MgAl9Zn1)	21	199	68	1.00E+06	90	74	-18%
AZ91 (MgAl9Zn1)	21	199	68	1.00E+09	73	49	-32%
AlSi9Cu	7	216	93	1.00E+05	117	98	-16%
AlSi9Cu	7	216	93	1.00E+06	87	82	-6%
AlSi5Cu3Mg0.4 T5	21	222	99	1.00E+06	88	85	-4%
AlSi5Cu3Mg0.4 T5	21	222	99	1.00E+09	67	56	-16%
AlCuMg2 T351	21	460	128	1.00E+06	200	204	2%
AlCuMg2 T351	21	460	128	1.00E+09	110	136	24%
AlZnMgCu1.5 T66	21	641	185	1.00E+06	240	304	27%
AlZnMgCu1.5 T66	21	641	185	1.00E+09	150	203	35%

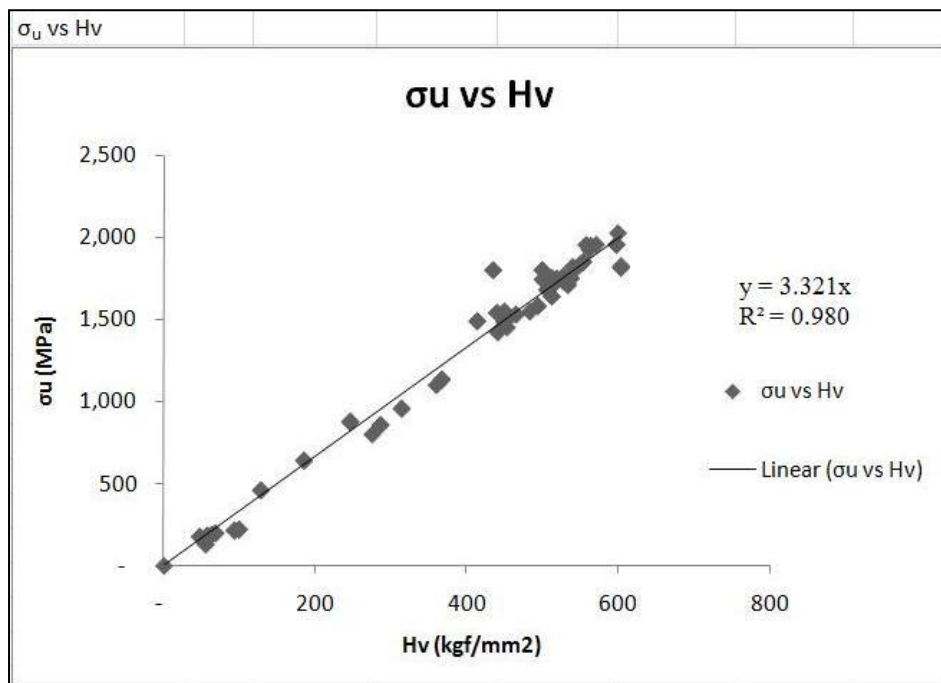


Figure A 1.  $\sigma_u$  vs Hv for steels and aluminium alloys